Materials Today Sustainability 31 (2025) 101212

Contents lists available at ScienceDirect

Materials Today Sustainability

journal homepage: www.journals.elsevier.com/materials-today-sustainability

Biobased epoxy resins obtained from resorcinol epoxy monomer and anhydrides

Angela Marotta [a,1,**], Cosimo Brondi [a,b,1,*], Mattia Sivero [a], Pierfrancesco Cerruti [c], Veronica Ambrogi [a], Alice Mija [d]

[a] Department of Chemical, Materials, and Production Engineering (UdR Naples, INSTM Consortium), University of Naples Federico II, Naples, Italy
[b] Department of Engineering and Science, Universitas Mercatorum, Rome, Italy
[c] Institute for Polymers, Composites and Biomaterials (IPCB), National Research Council (CNR), Pozzuoli, Italy
[d] Université Côte d'Azur, Institut de Chimie de Nice, 06100 Nice, France

ARTICLE INFO

Keywords:
Resorcinol
Imidazole
Biobased
Epoxy resins
Autocatalytic
Chemoreology

ABSTRACT

Design and development of high glass transition (T_g) biobased epoxy thermosets is a key challenge for several fields of applications. To this aim, in the present study diglycidyl ether of resorcinol (DGER) is proposed as a potentially biobased alternative to diglycidyl ether of bisphenol A (DGEBA) for the synthesis of high-performance epoxy resins. DGER is obtained by diglycidylation of resorcinol, an aromatic diol synthesized by fermentation of glucose or catechin. The curing process of DGER in the presence of various anhydrides as hardeners and several imidazole initiators is studied. The most efficient hardener/initiatior combination, which leads to the resin with the highest degree of reaction conversion and the highest glass transition (T_g > 100 °C) is further studied by chemorheological analysis, and a kinetic model for the crosslinking reaction is proposed. The conversion degree is evaluated by monitoring the disappearing of characteristic peaks of anhydride and epoxy rings in ATR-FTIR spectra collected at different curing temperature, as well as the appearance of the characteristic band of ester groups typically formed in epoxy/anhydride resins. By fitting the conversion data, the autocatalytic crosslinking mechanism is confirmed, and kinetic parameters are calculated. Also, the thermomechanical characteristics and chemical stability of DGER-based epoxy resins are evaluated, confirming the potential use of this epoxy thermosets when high mechanical and thermal properties are required.

1. Introduction

Petroleum-based polymers have been started to be used at industrial level for over a century, but the current geopolitical situation, coupled with dwindling oil and gas reserves, has led to an increase in the cost of oil-based raw materials. The global focus is therefore shifting the research and the subsequent production of more environmentally and economically sustainable materials. A sustainability-driven change in resource usage is especially urgent in the epoxy resins industry, as the use of diglycidyl ether of bisphenol A (DGEBA), the mainly used epoxy monomer in resin production, raises strong health and environmental concerns [1]. The transition to alternative, less harmful monomers is crucial for the future of the industry, and the research of alternatives among the plenty of bioderived molecules can help combine both material safety and sustainability.

One promising avenue for the development of sustainable epoxy resins is the choice of bio-based monomers derived from renewable resources such as plant oils, sugars, or lignin, both as epoxy monomers and hardeners [2]. Epoxidized vegetable oils are readily available among bioderived epoxides; yet, because of their high chain mobility, the resulting materials have poor mechanical characteristics. [3,4]. Yet, Di Mauro and coauthors have shown that by depending on the epoxide content in the epoxidized vegetable oil, and by a proper choice of the hardner, can be designed materials with a large variety of glass transition values [5–7]. Moreover, these materials shown shape memory abilities and are chemical recyclable, reprocessable and repairable (3R).

* Corresponding author. Department of Chemical, Materials and Production Engineering (UdR Naples INSTM Consortium), University of Naples Federico II, Naples, Italy.
** Corresponding author.
E-mail addresses: angela.marotta@unina.it (A. Marotta), cosimo.brondi@unimercatorum.it (C. Brondi).
[1] Equal contributions.

https://doi.org/10.1016/j.mtsust.2025.101212
Received 28 April 2025; Received in revised form 16 August 2025; Accepted 20 August 2025
Available online 23 August 2025

Table 1
Molecular structures of the selected epoxy molecule, anhydride hardeners, and initiators.

Name	Code	Chemical structure	Molar mass [g/mol]	Melting Temperature [°C]
Diglycidyl Ether of Resorcinol	DGER	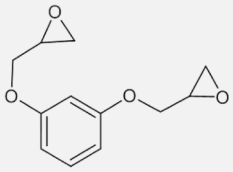	222.24	30
		Hardeners		
Itaconic Anhydride	IA	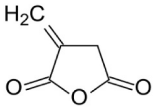	112.08	66
Maleic Anhydride	MA	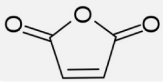	98.06	53
Succinic Anhydride	SA	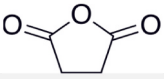	100.07	120
Phthalic Anhydride	PA	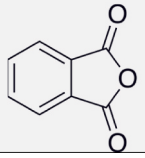	148.12	131
		Initiators		
N,N-Dimethylbenzylamine	DMBA	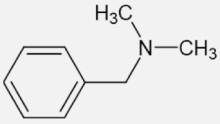	135.21	-75
1,2-Dimethylimidazole	1,2DMI	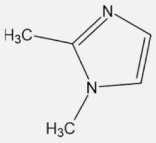	96.13	39
N,N-Dimethylaniline	DMAn	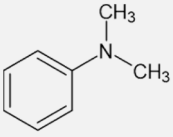	121.19	2
2,4,6-Tris(dimethylaminomethyl)phenol	DMP30	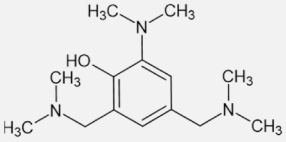	265.40	-20
1-Methylpiperazine	1MPIP	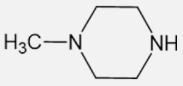	100.17	-6

On the other side, lignocellulosic biomass is a source of highly valuable aromatic molecules, such as eugenol [8–10], vanillin [11–13], tannic acid [14], with an aromatic structure that gives resins exceptional mechanical strength. However, to isolate these compounds from biomasses is laborious and then from a broad perspective, not very sustainable.

Within this context, resorcinol, an aromatic diol that can be readily synthesized by fermenting glucose or catechin [15], can meet the need for readily available and biobased aromatic molecules and the current market demands. Resorcinol can, indeed, be glycidylated into diglycidyl ether of resorcinol (DGER) [16] a molecule with a relatively low melting point and low cost, making it an optimum candidate to be a building block for high-performance biobased thermosets. At date, DGER have been photocured with an amine hardener by Nguyen et al. [17] showing good thermomechanical properties, or with eugenol glycidyl ether by

Modjinou and coauthors [18] resulting in a fully bio-based material with antioxidant properties and antibacterial activity against different strains. To achieve the highest sustainability as possible, of course, the use of biobased hardeners is preferable. In this regard, amine functionalized limonene and eugenol have been assessed for the crosslinking of DGER [19]. Fusteş-Dămoc and coauthors [16], instead, have proposed chitosan as crosslinker for DGER, obtaining a fully biobased epoxy resin with high storage moduli E' ~3.5−4.2 GPa and high crosslinking density. Dinu and coauthors [20] also combined the DGER with keratin or lignin, that showed a good reactivity with the bisepoxide. The designed fully biobased materials have shown glass transitions around 90 °C, low densities and overall good thermomechanical performances.

Amines, however, are intrinsically more toxic than anhydrides, which are attracting the interest of scientists as hardeners [21]. François et al. [22] tested six different biobased anhydrides as hardeners for both petrol- and bio-based epoxides, including DGER: the formulation was optimized using DGEBA as epoxy monomer, and with the selected formulation materials with good glass transition temperature and good hardness, measured by nanoindentation tests were obtained.

In this work, instead, the DGER curing process has been specifically studied in the presence of various anhydrides as hardeners and several imidazole initiators. The selected anhydrides were chosen according to their potential derivation from biomasses, with the aim of developing potentially fully biobased epoxy resins to replace the conventional fossil-derived DGEBA-based epoxies. The first phase of the study was conducted by analyzing the thermal behavior related to the curing process using Differential Scanning Calorimetry (DSC), focusing on the achievement of the best result in terms of physicochemical properties. More specifically, the main goal of this analysis was the achievement of the lowest pre-cure viscosity, the highest degree of reaction conversion, and the highest glass transition. The mixture that exhibited the most satisfactory results was further studied by chemorheological analysis, and a kinetic model for the crosslinking reaction was proposed, based on the conversion data obtained by means of ATR FT-IR spectroscopy. In addition, the thermomechanical characteristics and chemical stability of the DGER-based epoxy resins were also evaluated.

2. Experimental

2.1. Materials

The epoxy monomer, diglycidyl ether of resorcinol (DGER), was synthesized through an optimized glycidilation procedure [16]. Itaconic Anhydride (IA), Maleic Anhydride (MA), Succinic Anhydride (SA), Phthalic Anhydride (PA), N,N-Dimethylbenzylamine (DMBA), 1, 2-Dimethylimidazole (1,2DMI), N,N-Dimethylaniline (DMAn), Benzoxazole (BXA), 1-Methylimidazole (1MI), 2,4,6-Tris (dimethylamino--methyl)phenol (DMP30), and 1-Methylpiperazine (1MPIP) were purchased by Sigma-Aldrich (France) and used as received without further purification. Table 1 shows the molecular structures of the used compounds together with their physicochemical properties.

2.2. Sample preparation

Several samples were prepared by curing DGER with different anhydrides at a molar ratio of 1:2, varying type and amount of initiator. The sample preparation was made by mixing DGER with the initiator and then adding the previously mortar-ground anhydride hardener. The mixture was manually stirred until the anhydride was completely solubilized. Bulk materials were then prepared by pouring the mixture into silicon molds and cured according to the following program: 1 h at 75 °C + 1 h at 100 °C + 1 h at 140 °C + 1 h at 180 °C. A reference sample with DGEBA as epoxy monomer, MA as crosslinking agent and 1,2DMI as initiator, was prepared following the same protocol.

2.3. Characterization methods

Differential scanning calorimetric analysis (DSC) were conducted using a DSC 3 Mettler Toledo apparatus. The cure process was studied by performing dynamic measurements from 20 to 200 °C at a heating rate of 10 °C/min on 3 − 5 mg of freshly prepared samples placed in a 40 μL aluminum crucible. Further heating and cooling scans between 0 and 200 °C were performed at the same heating/cooling rate, to verify the cure completion and evaluate the glass transition (T_g).

A Thermo MARS III rheometer interfaced with an iN20 Nicolet FTIR spectrophotometer by a Rheonaut temperature controller was used to perform simultaneous rheological and attenuated total reflectance infrared spectroscopy (ATR FTIR) analysis. Chemorheological tests were performed on plate−plate geometries (with 20 mm in diameter and 1 mm of gap) at a fixed frequency (ω) of 10 rad/s and deformation (γ) in autostrain mode of 1.5 % ± 1.5 %. In the case of dynamic analysis, measurements were performed by varying the temperature from 40 to 200 °C and at heating rates of 2 °C/min and 10 °C/min. In the case of isothermal analysis, measurements were performed at five different temperatures: 80, 90, 100, 110, and 120 °C. The crossover temperature or time of the values of storage (G') and loss (G'') moduli were considered as gelation temperature (T_{gel}) or time (t_{gel}). Simultaneous ATR FT-IR analysis was performed by acquiring single beam spectra in the range of 4000−400 cm^{-1} with a resolution of 4 cm^{-1} and 16 scans. In this way, it was possible to monitor and quantify the contribution of the several functional groups involved in the curing process.

Subtraction spectra (i.e. the spectrum at $t = 0$ was subtracted from the spectra at different curing times) are performed to monitor and isolate the absorbance area under the characteristic peaks of the anhydride and ester carbonyl groups as their adsorption bands overlap during the process [23]. The anhydride as well as epoxy consumption and the ester formation were monitored by integrating the underlying absorbance area within the region between 1825 and 1749 cm^{-1}, the region between 920 and 850 cm^{-1}, and the region between 1749 and 1675 cm^{-1} respectively. In particular, the consumption of the anhydride and epoxy groups was evaluated by the following equations:

$$\alpha_{ANH} = \frac{A^t_{ANH} - A^\infty_{ANH}}{A^0_{ANH} - A^\infty_{ANH}} \quad (1)$$

$$\alpha_{EPO} = \frac{A^t_{EPO} - A^\infty_{EPO}}{A^0_{EPO} - A^\infty_{EPO}} \quad (2)$$

where the subscripts ANH and EPO represent respectively the anhydride and epoxy groups, while the superscripts 0, ∞ and t represent respectively the initial time, final time and the current time. In addition, the following equation was used to evaluate the relative ester conversion:

$$\alpha_{EST} = \frac{A^t_{EST}}{A^\infty_{EST}} \quad (3)$$

where A^t_{EST} and A^∞_{EST} indicate the integrated absorbance area from subtracted spectra at the current curing time t and at a final plateau value, respectively.

Dynamic mechanical analysis (DMA) was performed by using a DMA Mettler Toledo apparatus on specimens with dimensions of approximately 49 × 7 × 3 mm^3 (length × width × thickness). Samples were analyzed in the temperature range −100 °C to 300 °C at a heating rate of 3 °C/min. The frequency and the amplitude were respectively 1.0 Hz and 20 μm using a three-point bending clamp. From these measurements, in addition to the storage modulus (E'), the loss modulus (E''), and the damping factor ($tan\ \delta$), the crosslink density (ν) and the molecular weight between crosslinks (M_c) were calculated using the following equations, respectively:

$$\nu = \frac{E'}{3R(T_g + 50)} \quad (4)$$

$$M_c = \frac{3\rho R(T_g + 50)}{E'} \tag{5}$$

where $T_g + 50$ is the glass transition temperature in Kelvin, evaluated as the temperature at which the maximum value of *tan* δ is recorded, plus 50 K, R is the ideal gas constant, ρ is the cured resin density and E' is the storage modulus evaluated at $T_g + 50$. The density ρ was empirically calculated by measuring the volume and weight of specimens used for the DMA test.

Hardness tests were carried out following the standard ISO 7619-1, ASTM D2240, and ISO 868. A Shore D durometer (Zwick Roell 3116 Hardness Tester) was used with an applied load force of 50 N ± 0.5 N.

Tensile tests were conducted according to ISO 527-141 and ASTM D638-0842 by using an Instron 3365 (Norwood, MA, USA) with a speed of 10 mm/min, on specimens of approximately 75 × 10 × 2 mm^3 (length × width × thickness). Tensile parameters as the materials strength (σ) and the Young's modulus (E) were evaluated as an average of tests performed on five different specimens.

The amount of absorbed water, W_a, was determined according to standard ASTM D57034 on rectangular samples with dimensions of 10 × 8 × 4 mm^3 (length × width × thickness). Samples were dried in an oven at 50 °C for 24 h and then weighed with a ML3002T Mettler Toledo precision balance. Therefore, specimens were entirely immersed in distilled water at room temperature for different times. Once removed from the water, they were carefully wiped with filter paper and their mass was measured. The water absorption was calculated by using the following equation:

$$W_a = \frac{W_t - W_0}{W_0} \tag{6}$$

where W_0 represents the initial mass of dried sample and W_t the mass of the wet sample after immersion in water.

The gel content (GC) of the cured samples was determined by using the solvent extraction method in different solvents. The analyzed samples, with dimensions of 20 × 8 × 4 mm^3 (length × width × thickness), were dried in an oven at 50 °C for 24 h and later immersed in several solvents, namely acetone, toluene, methanol, acetonitrile, chloroform and tetrahydrofuran. Therefore, the samples were wiped at different times with filter paper and weighed with a ML3002T Mettler Toledo precision balance. The GC was calculated by using the following equation:

$$GC = \frac{W_s}{W_0} \tag{7}$$

where W_0 represents the initial weight of dried sample, W_s is the mass of wet sample after immersion.

2.4. Kinetic modeling of the curing reaction

In case of isothermal analysis, the functional dependence of the conversion rate can be regarded as the product of two functions that comprise their respective dependence on the temperature T and the conversion degree α:

$$\frac{d\alpha}{dt} = k(T)\, f(\alpha) \tag{8}$$

where $k(T)$ is the kinetic constant that encloses the relationship with the temperature by assuming the well-known Arrhenius function, while $f(\alpha)$ is the function that expresses the reaction mechanism of the curing process. The activation energy of the curing process represents the minimum energy required to activate the reactant molecules so that they may undergo chemical transformation [24]. Under this perspective, this parameter can be regarded, according to the transition state theory, as the energy difference between the initial molecules at their initial configuration and the corresponding transition molecules in their activated configuration [25]. Therefore, the Arrhenius equation is suitable to describe the activation energy enclosed in the rate constant and can formally disregard the concentration of the reactants:

$$k(T) = A\, e^{-E_a/RT} \tag{9}$$

where A is the pre-exponential factor, R is the universal gas constant, T is the temperature and E_a is the activation energy. On the other hand, the reaction model reflects the reaction mechanism and, in our case, is often described by a n^{th}-order (eq. (10)) or an autocatalytic (eq. (11)) process (Kamal's equation) [26,27]:

$$f(\alpha) = (1 - \alpha)^n \tag{10}$$

$$f(\alpha) = \alpha^m\, (1 - \alpha)^n \tag{11}$$

In the first case, the order kinetics indicates a reaction rate proportional to the n exponent of the reactant concentration and, therefore, assumes that only one reaction occurs during the curing process and leads to some limitations as more simultaneous reactions may take place [28,29].

As it regards the kinetic expression of the reaction rate, in their preliminary work, M.R. Kamal and S. Sourour [30] showed that the isothermal cure data could be correlated with temperature and time by employing the following kinetic equation:

$$\frac{d\alpha}{dt} = k\, \alpha^m\, (1 - \alpha)^n \tag{12}$$

where m and n were the reaction orders independent of the temperature, while k was the rate constant dependent on the temperature. Subsequently, M.R. Kamal [31] effectively reported that the cure of both epoxy and unsaturated polyester systems could be described by the following kinetic equation:

$$\frac{d\alpha}{dt} = (k_1 + k_2\, \alpha^m)\, (1 - \alpha)^n \tag{13}$$

where k_1 and k_2 were the rate constants, m and n were the usual reaction orders independent of the temperature. According to the first autocatalytic model (equation (12)), the conversion rate is zero or, at least, very small at the beginning of the process and it attains a maximum value at intermediate conversion values. The modified Kamal equation (second autocatalytic model, equation (13)) takes into account the possibility that the initial rate of autocatalytic reactions may not be necessarily zero [26,32]. Therefore, while the modified form of the Kamal equation accounts also for this eventuality, m and n are still retained as reaction orders [32,33]. For this reason, in this work experimental data were fitted by autocatalytic model, where the exponent m describes the order of the initiation step and the exponent n describes the order of the autocatalytic step [28,29]. The equation can be formulated in the form of separation of variables:

$$\frac{d\alpha}{\alpha^m\, (1 - \alpha)^n} = k(T)\, dt \tag{14}$$

In this way, experimental data can be analyzed by the reaction mechanism in its integral form:

$$g(\alpha) = \int \frac{d\alpha}{\alpha^m\, (1 - \alpha)^n} = \int k(T)\, dt = k(T)\, t \tag{15}$$

3. Results and discussion

Several curing agents suitable for the epoxy cross-linking process are commercially available and mainly include amines, anhydrides, and dicarboxylic acids, whose choice depends on key properties such as curing time, pot life, viscosity, chemical, mechanical, and thermal resistance [34]. Under this perspective, anhydrides represent a more

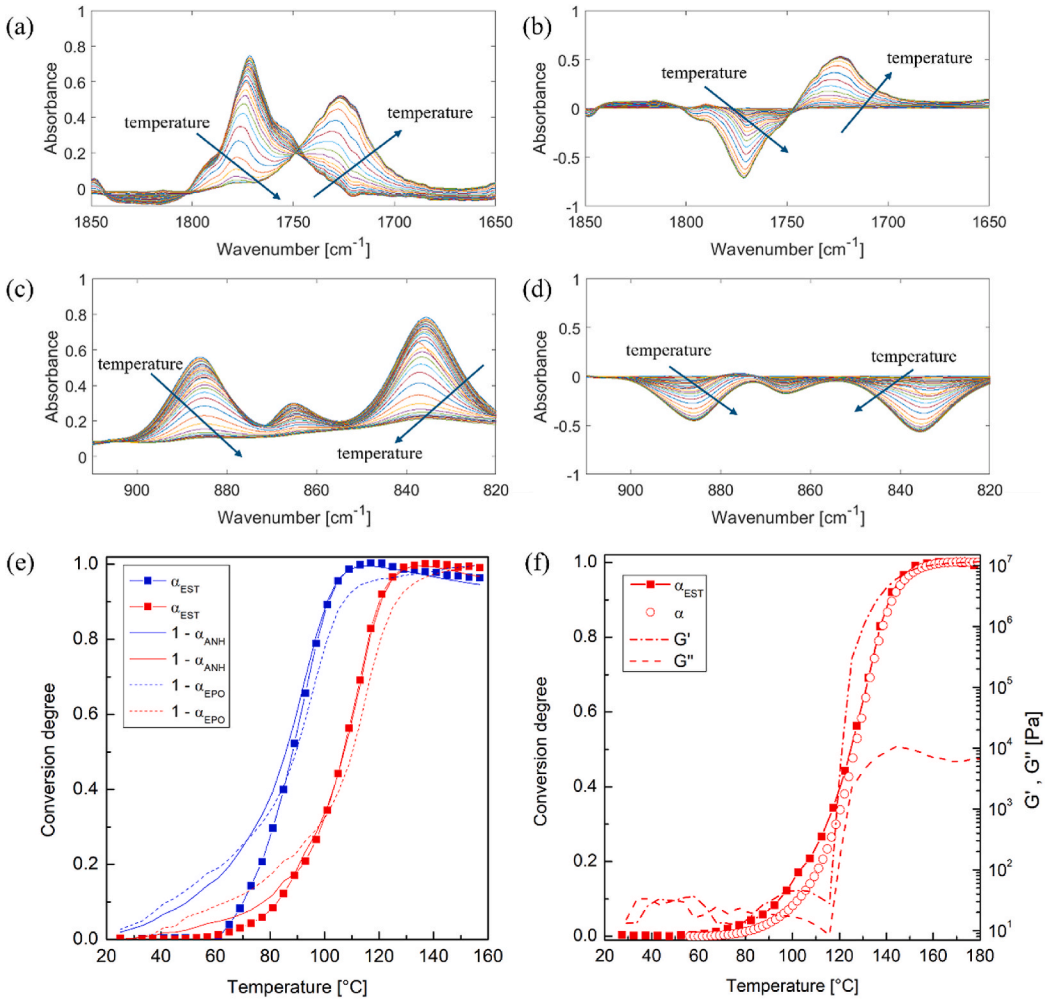

Fig. 1. Evolution of ATR FTIR spectra (left side of the panel) and difference spectra (right side of the panel) of DGER-MA-1,2DMI system heated at 10 °C/min in (a and b) the regions 1825-1749 cm^{-1} and 1749-1675 cm^{-1} showing anhydride consumption and ester formation, as well as (c and d) 920-850 cm^{-1} range, showing epoxy ring opening. For each heating scan, the temperature range was from 25 °C to 160 °C. (e) Consumption and conversion degrees of reactants and product as function of temperature at 2 °C/min (blue curves) and 10 °C/min (red curves) as measured by ATR FTIR; (f) Conversion degree of the ester group monitored by ATR FTIR, and conversion degree monitored by DSC (left axis) compared to storage and loss moduli monitored by rheometer (right axis). All data are obtained at 10 °C/min.

sustainable alternative, compared to amines, yet providing good mechanical performances to the final product [35]. Therefore, several anhydrides and varying types and amounts of initiators were tested to investigate the curing behavior of DGER, with the aim of achieving the highest degree of conversion and the highest glass transition temperature of the resulting thermoset. Related results of this extensive experimental campaign are reported in the supporting information (S1 and S2) of this manuscript.

3.1. Curing behavior and kinetic evaluation of the DGER-MA-1,2DMI

At the beginning of this study, the DGER-IA system was first chosen as a model formulation, and different initiators at 1 wt%, including DMBA, 1,2DMI, DMAn, BXA, 1MI, DMP30, and 1MPIP were studied by DSC in non-isothermal mode (see SI). Several parameters such as enthalpy of reaction (ΔH_r), initial (T_{in}), ending (T_{end}), peak (T_{peak}) temperatures, as well as the glass transition (T_g) after curing were evaluated (see Table S1 in SI). Among all the tested initiators, mixtures with 1,2DMI, DMP30, and 1MPIP exhibited the best performance in terms of high T_g, narrow temperature range of reaction ($\Delta T = T_{end} - T_{in}$) and high ΔH_r (Table S2 in SI). The 1,2DMI was therefore selected for the main investigation as the initiator which resulted in the highest T_g, and several compositions were tested: 0.5 wt%, 1.0 wt%, 1.5 wt%, and 2.0 wt%. Accordingly, 1.5 wt% 1,2DMI was selected due to a balance between enthalpy of reaction and glass transition temperature, and the narrowest temperature range of reaction ($\Delta T = T_{end} - T_{in}$).

Subsequently, the reactivity of DGER with different anhydrides was evaluated. In particular IA, PA, MA and SA, in a 1:2 epoxy to anhydride molar ratio (1:1 equivalent ratio) were selected. With regard to the hardener choice, IA and MA were characterized by a complete miscibility with DGER at room temperature, while PA and SA formed viscous systems difficult to process as they were soluble only at temperatures higher than 50 °C. MA was finally chosen as the DGER-MA system exhibited the most controllable reaction process between its reactants in terms of sharp and monomodal curing peak as well as high enthalpy value (see Table S3 in SI).

Overall, from the study of the role of different parameters, such as the nature and the amount of initiator, nature of the anhydride on the thermal properties of the different epoxy resin formulations (see SI), the most promising system was DGER-MA-1,2DMI at 1.5 wt%. The latter was then to be further characterized to assess curing kinetics and chemical-physical and mechanical properties.

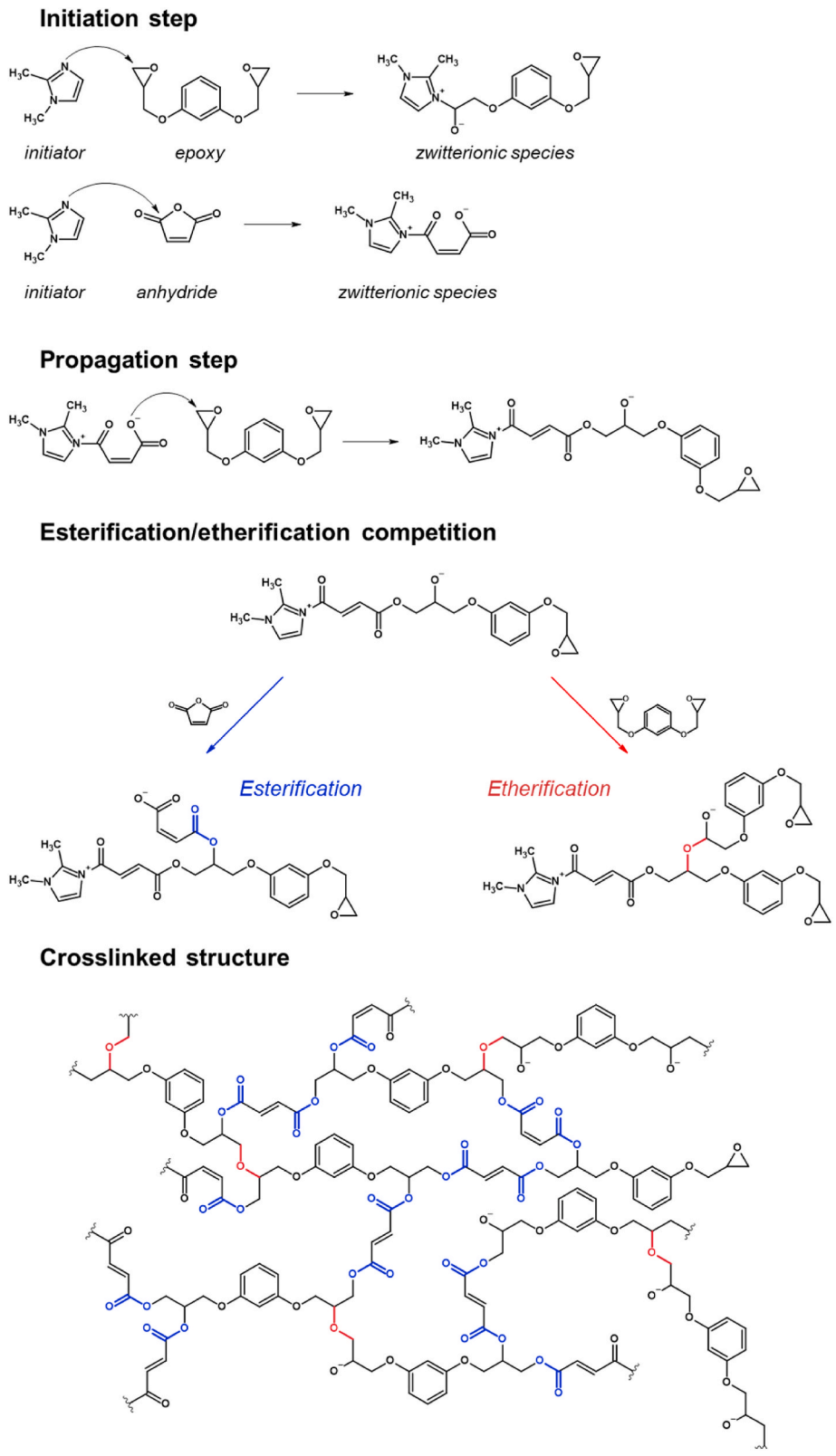

Scheme 1. Schematic representation of the curing reaction steps involving DGER and MA in presence of 1,2DMI.

3.1.1. Chemorheological analysis in non-isothermal mode

In the first series of experiments, the non-isothermal conversions of the DGER-MA reacting system in the presence of 1,2DMI were evaluated by collecting FTIR spectra upon heating the sample on the rheometer stage. In this way, the chemical transformation of the reacting system was monitored simultaneously to its viscoelastic behavior. Fig. 1 depicts the temperature-dependent evolution of the FTIR spectra collected upon curing DGER-MA-1,2DMI. In particular, the spectral regions at 1825-1749 cm^{-1}, 1749-1675 cm^{-1} (Fig. 1a and b), and 920-850 cm^{-1} (Fig. 1c and d) were used to monitor anhydride consumption, ester formation

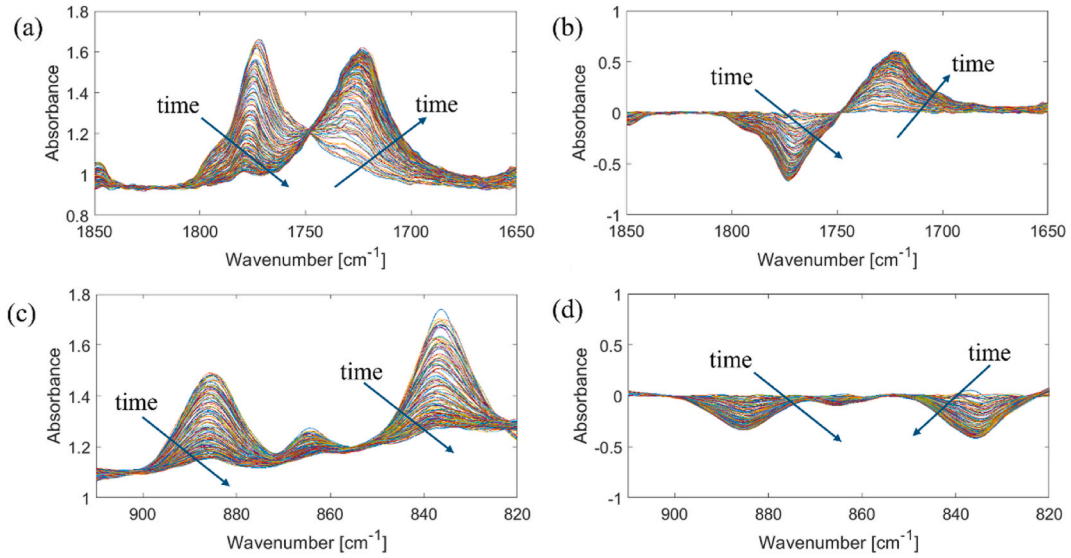

Fig. 2. Evolution of ATR FTIR spectra (left side) and difference spectra (right side) of DGER-MA-1,2DMI system at 80 °C in (a and b) the regions 1825-1749 cm^{-1} and 1749-1675 cm^{-1} showing anhydride consumption as well as ester formation and in (c and d) the region 920-850 cm^{-1} showing epoxy ring opening.

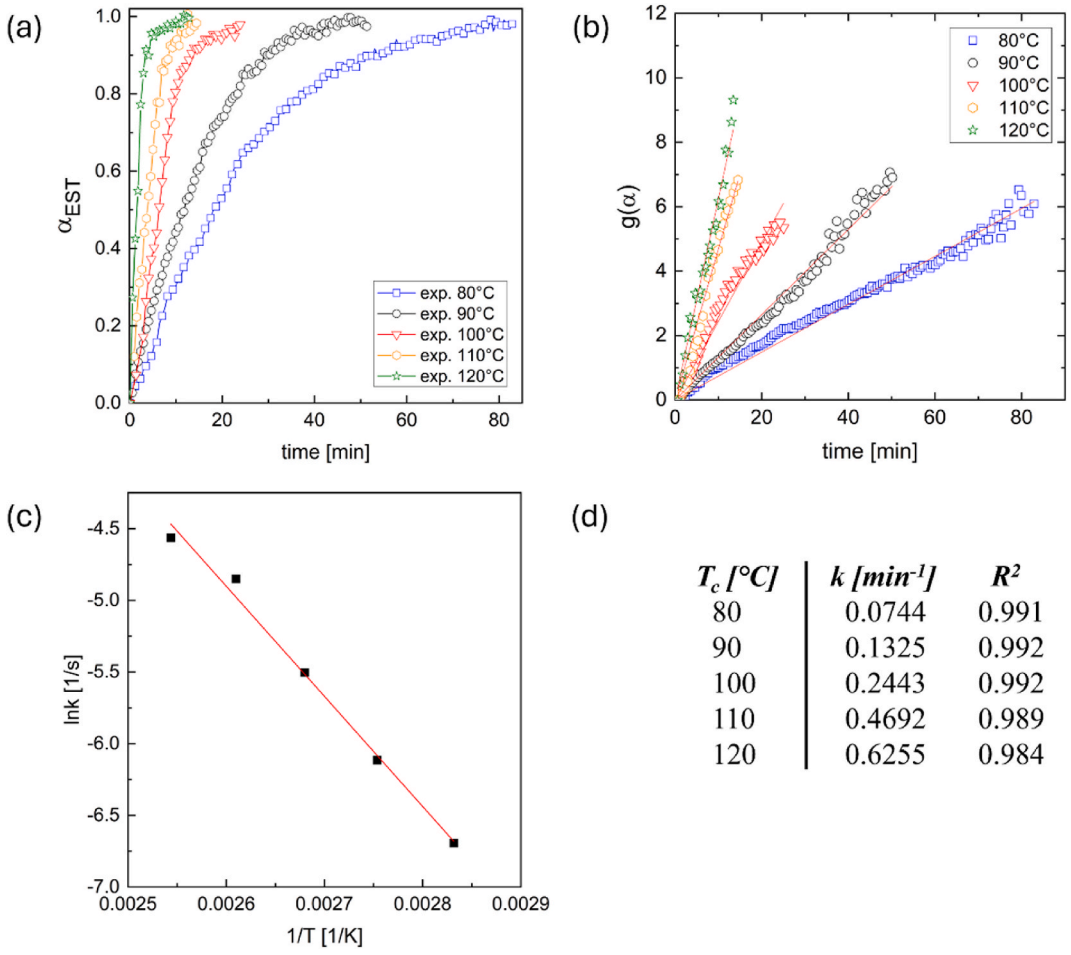

T_c [°C]	k [min^{-1}]	R^2
80	0.0744	0.991
90	0.1325	0.992
100	0.2443	0.992
110	0.4692	0.989
120	0.6255	0.984

Fig. 3. Analysis conducted on isothermal ATR FTIR spectra to gather insight about the reaction mechanism: (a) conversion degree, α, as function of the curing time and obtained according to equation (3) (lines are guide to the eye); (b) fitting procedure conducted on the reaction mechanism in its integral form $g(\alpha)$ obtained according to equation (15) (lines are linear fitting); (c) linear fitting of the logarithm form of the Arrhenius equation. (d) Kinetic parameters obtained by least square fitting of the reaction mechanism $g(\alpha)$ for the curing system at several curing temperatures.

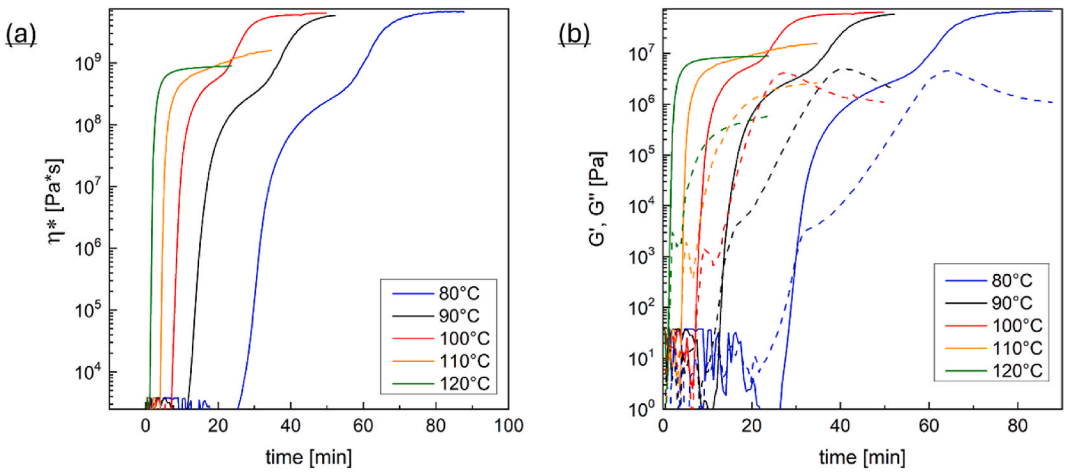

Fig. 4. Experimental results from rheological tests: (a) viscosity as function of the curing time; (b) storage (G', solid line) and loss (G'', dash line) moduli as function of the curing time.

and epoxy ring opening, respectively. In the 1800-1700 cm^{-1} range, two overlapping peaks are noted, related to the C=O stretching. The peak located at 1780 cm^{-1} decreases upon curing, as is due to anhydride consumption, while the absorption at 1730 cm^{-1} increases due to ester group formation [36,37]. The complete curing process is evidenced from the disappearance of the anhydride and epoxy ring bands as well as the plateau attained by the ester peak.

The absorbance area was used to evaluate the anhydride and epoxy consumption as well as the ester formation, according to eqs. (1)–(3). For both non-isothermal heating experiments, Fig. 1e shows that at temperatures lower than 60 °C anhydride and epoxy groups conversion occurs, while ester formation is still not detectable. This evidence may be attributed to the initiation process, in which anhydride and epoxy react with 1,2DMI forming zwitterion species (see section S3 in SI). Subsequently, during the propagation step (T > 60 °C), the ester group starts forming due to the reaction of the zwitterions formed in the initiation step with anhydrides and epoxides (Scheme 1) [37].

Several authors focused on the temporal evolution of functional groups such as those of ester as well as epoxy and anhydride as measured by FTIR in non-isothermal mode. Rebei et al. [38] studied the accelerating effect of imidazolium metal-based ionic liquids in comparison to reference catalysts such as 1-methylimidazole (1-MI) and 1-butyl-3-methylimidazolium chloride (1-B-3-MICl). In that study, the epoxy-anhydride (DGEBA-methylhexahydrophtalic anhydride [MHHPA] system) copolymerization mechanism was investigated by means of Near-infrared (NIR) spectroscopy in non-isothermal mode. In the case of the 1-MI, it was reported that the ester formation seems to exhibit an induction temperature (ca. 80 °C) for its formation when compared to anhydride consumption. In the present case, interestingly, at temperatures of 88 °C and 108 °C for heating runs at 2 and 10 °C/min respectively, the curves related to ester formation and the anhydride/epoxy proceed at the same conversion rate, suggesting that the growth of the network mainly occurs through an alternating copolymerization mechanism [37]. At temperatures of 115 °C and 135 °C for 2 °C/min and 10 °C/min, respectively, and a conversion extent of approximatively 1, the kinetic curves of the reactants and product approach simultaneously the final conversion value (Fig. 1e).

The alternating copolymerization mechanism is also confirmed by data reported in Fig. 1f. In this case, conversion degree obtained from ATR FTIR spectra (ester group) and from DSC data (evaluated according to the method proposed in Refs. [39,40]) are plotted together with storage and loss moduli (G' and G'', respectively) obtained from rheological measurements (all measurements performed at 10 °C/min). It is noticed that the conversion curves nicely overlap over the examined range of temperature, suggesting that the reaction enthalpy evolves with the ester formation [37]. Regarding the rheological behavior, three stages are noticed: at low temperature (up to 110 °C), the uncured resin exhibits very low moduli values, which are below the detection range of the instrument. As the temperature reaches values above 120 °C, a remarkable increase in both storage and loss moduli is observed, with G' values (10^7 Pa) being three orders of magnitude greater than G'' values (10^4 Pa), thus indicating the transition from a viscous to an elastic behavior. Interestingly, the abrupt increase in G′ takes place only when the conversion extent of ester groups achieves a value of 0.3, indicating that the polymer crosslinking occurs above this threshold value and an interconnected macromolecular structure percolates the entire sample. However, from non-isothermal FTIR-rheological measurements no information on the crossover of G' and G'' curves could be obtained. Therefore, to gather further insight into the reaction mechanism of the system under study, isothermal analysis was performed in the temperature range between 80 and 120 °C, as discussed in the next section.

3.1.2. *Chemorheological analysis in isothermal mode*

Fig. 2 depicts the evolution of the FTIR spectra collected upon curing DGER-MA-1,2DMI during the rheological isothermal measurements at 80 °C, in the 1825-1749 cm^{-1}, 1749-1675 cm^{-1} (Fig. 2a and b), and 920-850 cm^{-1} (Fig. 2c and d) spectral regions. Analogously to non-isothermal tests, two overlapping peaks related to the C=O stretching are present, due to anhydride consumption (1780 cm^{-1}) and ester formation (1730 cm^{-1}) [36,37]. Moreover, the peak associated with the epoxy ring (872-972 cm^{-1}) completely disappears upon curing, confirming that the process attains its final extent of cure.

The ester conversion was evaluated according to equation (3) for each isothermal run, as reported in Fig. 3a. For higher curing temperatures (T_c, i.e. the temperature at which the isothermal analysis is conducted), the reaction rate increases, and therefore a higher curing degree is attained in a shorter time. The coefficients of the kinetics order (m and n) that trivially confer a linear behavior were gathered and the reaction rate data were simultaneously fitted according to equation (15) by an integral method with minimization of the least square error function. The resulting fitting parameters are reported in Fig. 3b. Overall, the fitting curves are in good agreement with the experimental data, and thus are well described by the autocatalytic model, typical of anhydride-cured epoxy resins [37,39]. The best-fitting values obtained for the kinetic parameters at the several curing temperatures are reported in Fig. 3. Exponents m and n were respectively equal to 0.6 and 1.1, with m lower than n, indicating that the autocatalytic step is predominant with respect to the initiation step [40,41]. A further analysis was conducted to retrieve parameters related to the rate constant k (obtained as the slope of each curve reported in Fig. 3b). As it is usually performed in case

Table 2
Maximum value of elastic modulus (G'_{max}), and gelation time (t_{gel}) evaluated by rheological tests at different curing temperatures (T_c).

T_c [°C]	G'_{max} [MPa]	t_{gel} [min]
80	68	26
90	58	11
100	65	7
110	15	4
120	8	0.9

of Arrhenius-type processes, the logarithm of the rate constant was plotted against the inverse of temperature (Fig. 3c), providing the values of the activation energy, E_a, (63.89 kJ/mol) and the pre-exponential factor A (3.54×10^6 s^{-1}) in good agreement with values already observed for similar epoxy/anhydride thermosets [41,42].

Results from the rheological tests of all the isothermal heating experiments are reported in Fig. 4. Fig. 4a shows the complex viscosity curves, which feature a two-step growth for curing temperatures of 80, 90 and 100 °C, while at higher temperatures a single step takes place. Accordingly, G' and G'' (Fig. 4b) follow the same two-step trend at lower temperatures. Moreover, the gel time, corresponding to the G′-G″ crossover, and the maximum values of G', decrease with the temperature (Table 2).

To shed light on this complex behavior, isothermal DSC runs were performed on the same system at T_c of 80 and 100 °C. The relative thermograms (Fig. 5a) show that the exothermic peaks at 80 °C featured a bimodal pattern, that became less pronounced as the temperature was increased to 100 °C. Therefore, the bimodal behavior observed in both rheological and DSC measurements is unambiguously peculiar to the system cured within this range of temperatures. Focusing on the cure behavior of epoxy-anhydride systems initiated by imidazole-based compounds, Park et al. [43] isothermally cured an epoxy-anhydride system with an imidazole derivative at various temperatures, for both stoichiometric and epoxy-rich formulations. When reporting residual exothermic peaks for samples cured at 75 °C, a bimodal pattern was noted during the initial stages of the curing process. This occurrence was attributed to two subsequent cure reaction steps, namely esterification followed by etherification. Other authors also reported the occurrence of etherification when those types of imidazoles interact with the epoxy ring [44]. Likewise, we may infer that the two-step mechanism observed from the rheological experiments is attributed to these two curing steps (Scheme 1). Isothermal ATR FTIR were also monitored to gain further insight on this aspect, and the appearance of a broad aliphatic ether band was detected in the 1180-1110 cm^{-1} region [44], as displayed in

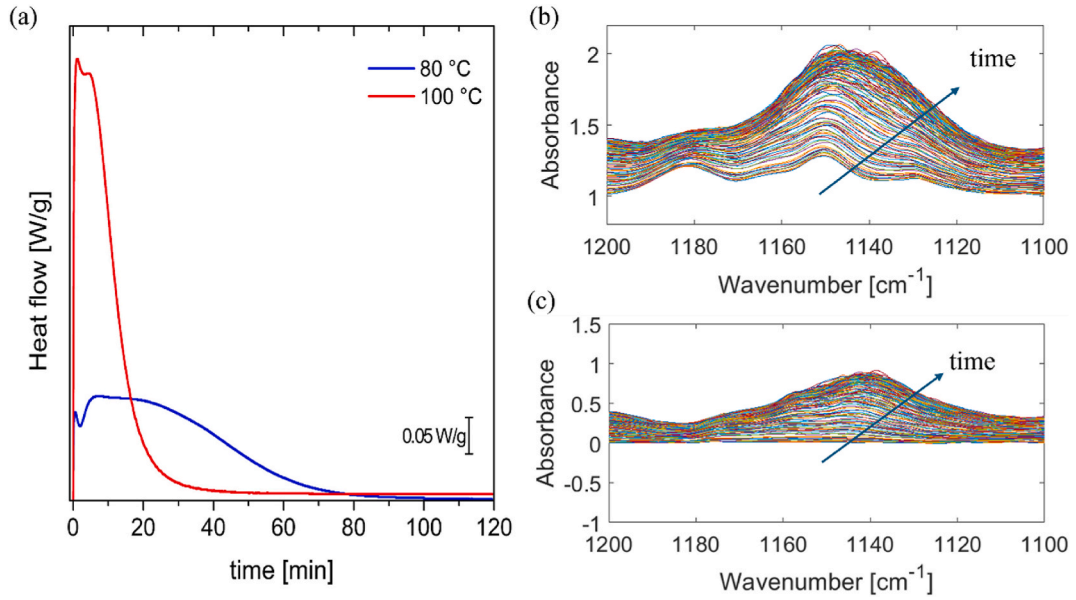

Fig. 5. (a) DSC thermograms related to the isothermal curing exotherm peaks of DGER-MA-1,2DMI at 80 °C and 100 °C. (b) Evolution of ATR FTIR spectra, and (c) difference spectra of DGER-MA-1,2DMI system at 80 °C in the 1180-1100 cm^{-1} range, showing the formation of a broad aliphatic ether band.

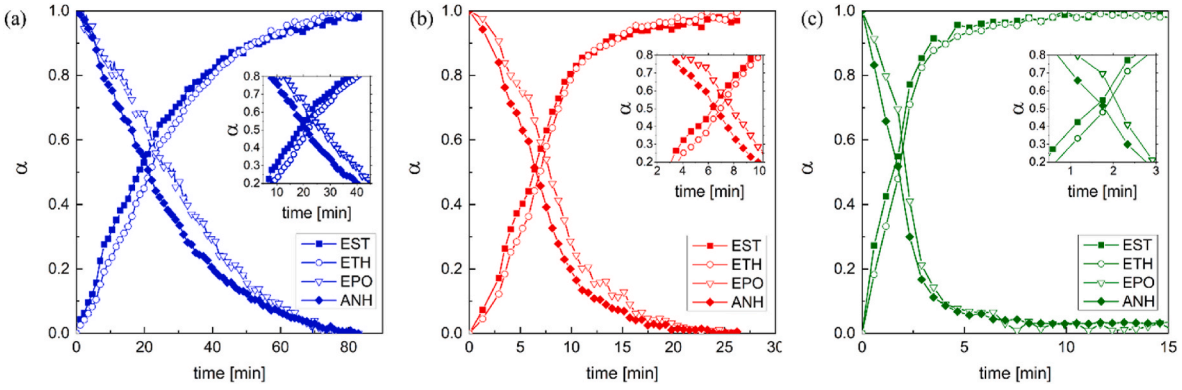

Fig. 6. Relative epoxy and anhydride conversions as well as ester and ether formations as function of the curing time at (a) 80 °C, (b) 100 °C and (c) 120 °C. Lines are guide to eye.

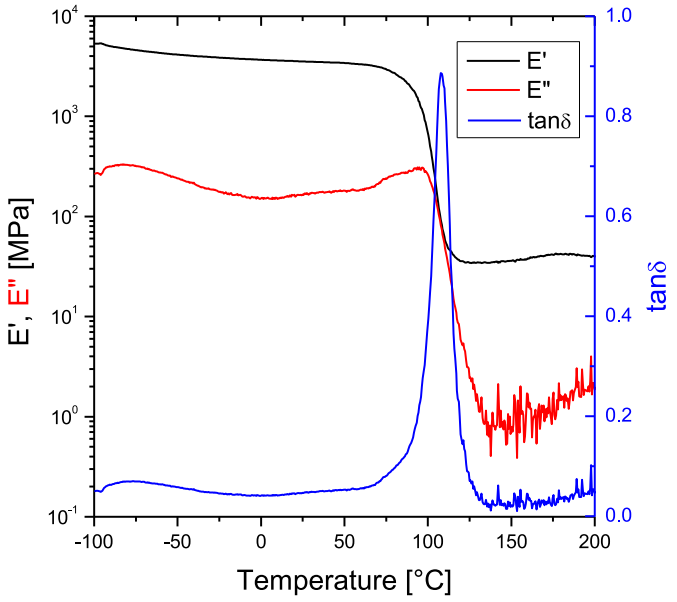

Fig. 7. Loss modulus (E'), storage modulus (E'') and damping factor (tan δ), for DGER-MA-1,2DMI, evaluated by DMA.

Fig. 5b for a curing temperature of 80 °C.

The evolution of the ether band was normalized as previously shown for the ester formation (Fig. 3a) to gain insight on the formation of crosslinked structures. The conversion profile was compared to the ester formation and epoxy and anhydride conversions (as evaluated from the ATR FTIR spectra) as reported in Fig. 6 at 80 °C, 100 °C, and 120 °C. At T = 80 °C, the anhydride conversion was faster than that of epoxide, suggesting that the imidazole favorably interacts with the former group at the early stage of the curing process [45,46]. However, this chemoselectivity was less evident at higher curing temperatures.

As expected, the rate of ester formation was faster than that of the ether formation due to the conversion of the secondary OH groups, supporting the view that the first step in the curing process is the to the alternate co-polymerization mechanism, as also reported by Park et al. [39]. After a certain curing time, the ether formation curve intersected that of ester formation. In particular, at 80 °C the crossover occurred after 50 min, which actually corresponded to the beginning of the second step growth in the viscosity curve reported in Fig. 4a. This finding was also accompanied by the observation of a lower degree of conversion of epoxy rings compared to the anhydride compound near the end of cure (Fig. 6a). Indeed, during the final reaction times, homopolymerization is further enhanced, and etherification is mainly responsible for the build-up of the curing process at 80 °C [43]. At 100 °C (Fig. 6b), a similar behavior was noted, however the conversion curves of epoxy and anhydrides, and those relative to ester and ether linkages approached each other earlier. In fact, esterification and etherification occurred in a shorter time, with an anticipated evidence of the bimodal behavior, as also observed from the rheological tests (Fig. 6). A further increase in curing temperature entails complete overlapping of the conversion curves, suggesting the simultaneous occurrence of the esterification and etherification processes, consistent with the switch of the curing process from a bimodal to a unimodal behavior (Fig. 6c).

3.2. Physico-chemical and mechanical properties of DGER-MA-1,2DMI

In the light of the above reported results, a multistep curing protocol was employed for bulk resin preparation, according to the protocol reported in the Experimental section. The resulting cured samples were first characterized in their mechanical performance, by means of DMA, shore harness and tensile tests. The DMA test conducted on DGER-MA-1,2DMI from −100 to 250 °C allowed to identify the different temperature-dependent relaxation processes (Fig. 7). In particular, the T_g was identified at 100 °C, a temperature consistent with the results of DSC analyses reported above, and with literature data for DGER cured with a commercial amine hardener [17]. Furthermore, the material showed a sub-glassy transition near −80 °C, which for anhydride-cured epoxy resins is mainly controlled by the anhydride chain segments rather than the epoxy chains [47]. DMA analysis was also used to evaluate the crosslinking density (ν) and the molecular weight between

Table 3
Mechanical performance of DGER-MA-1,2DMI and DGEBA-MA-1,2DMI bulk samples, compared to literature data for biobased epoxy resins cured with MA.

	T_g [°C]*	Hardness [Shore D]	E [GPa]	σ_{max} [MPa]	ϵ_{max} [%]	Reference
DGER-MA-1,2DMI	100	76.4 ± 8.3	1.4 ± 0.1	97.7 ± 5.3	9.2 ± 0.7	This work
DGEBA-MA-1,2DMI	155	N.A.	0.8 ± 0.1	45.5 ± 14	10.7 ± 1.3	This work
Bio-based epoxy						
GEEA[a]-MA	106	N.A.	1.9 ± 0.2	42.4 ± 1.1	3.1 ± 0.5	Huang 2014
BOMF[b]-MA	34	N.A.	0.4 ± 0.1	14.1 ± 1.0	17.0 ± 2.0	Faggio 2023
DGEBF[c]-AESO[d]-MA	N.A.	62.7	2.4	32.00	1.02	Kocaman 2016

*Evaluated as the temperature of the *tan δ* peak.
[a] Glycidyl Ester of Eleostearic Acid.
[b] 2,5-Bis [(Oxiran-2-ylmethoxy)Methyl]Furan.
[c] Diglycidyl Ether of Bisphenol F.
[d] Acrylated Soybean Oil.

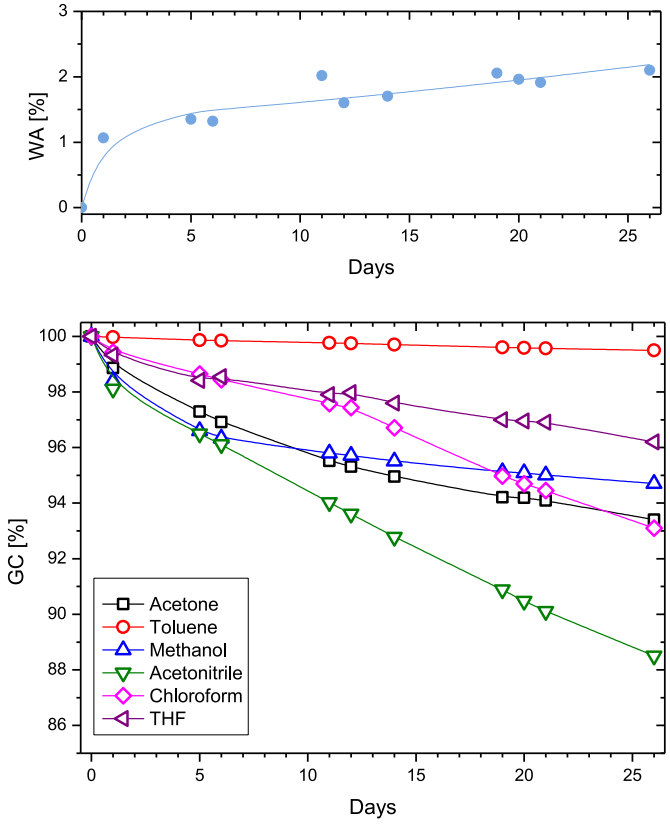

Fig. 8. (a) Water absorption (WA) and (b) gel content (GC) of DGER-DMA-1,2DMI.

crosslinks (M_c), according to equations (4) and (5). In details, values of $\nu = 3.7 \times 10^{-3}$ mol/cm^3, and $M_c = 373$ g/mol ($\rho = 1.27 \pm 0.3$ g/cm^3) were calculated. The crosslinking density values of the proposed material is significantly higher than those reported for both petrol-derived [48] and bioderived [49] epoxy/anhydride resins. Accordingly, the M_c value, is lower than data reported by literature [50,51]. These values hint the good mechanical and chemical properties of the material, hereafter reported.

In Table 3 the mechanical properties of DGER-MA-1,2DMI are summarized, and compared to the DGEBA-based analogous resin, DGEBA-MA-1,2DMI. Even though the T_g of the DGEBA-based epoxy resin is higher compared to the DGER-based resin, the material shows lower values of elastic modulus and strain at break and a comparable deformation at break. Different bioderived epoxy molecules, crosslinked with the same anhydride, lead to resins with worse mechanical resistance [4,52,53]. DGER, on the other hand, allowed to obtain good tensile properties by curing with MA, especially as concerns stress and ductility. The excellent hardness exhibited by resorcinol based resins are related to the presence of the aromatic ring into the crosslinked structure [53].

A further characterization on DGER-MA-1,2DMI was conducted to evaluate its chemical stability in different solvents. The extent of water adsorption and gel content (GC) as a function of time were evaluated by gravimetric methods and summarized in Fig. 8. In the early 24 h, the water absorption rate was high, and then significantly decreased. After 26 days a swelling value of about 2 % was recorded. As for GC, its trend with time was strongly related to the solvent nature. For all solvents, at least 90 % of sample was recovered after 26 days, indicating a highly crosslinked material. In particular, the thermoset was completely insoluble in methanol (GC of about 100 %), showed good stability in toluene, methanol, tetrahydrofuran, and chloroform (about 95 % gel content), and was less stable in acetonitrile, for which a GC of 89 % was observed after 26 days of soaking.

4. Conclusions

In this work, diglycidyl ether of resorcinol (DGER) was cured with four different anhydrides and several imidazole initiators. The cure reaction was studied by DSC and the best formulation, in terms of reaction conversion degree, pre-cure viscosity and T_g, was found to be the one cured with maleic anhydride in presence of 1.5 wt% of 1,2-dimenthylimidazole. The cure mechanism of this resin was studied by chemo-reological analysis, and conversion degree was evaluated by monitoring the evolution of ATR FTIR spectra as a function of the curing temperature. Data analysis confirmed that the epoxy/anhydride crosslinking reaction proceeds through an alternate copolymerization reaction, which followed an autocatalytic mechanism. Further, bulk samples obtained with the selected formulation showed good mechanical properties, with a shore D hardness of 76, elastic modulus of 1.4 GPa and a tensile strength of 98 MPa, as well as low moisture absorption and good organic solvent resistance.

CRediT authorship contribution statement

Angela Marotta: Writing – review & editing, Writing – original draft, Investigation, Formal analysis, Data curation. **Cosimo Brondi:** Writing – review & editing, Writing – original draft, Investigation, Formal analysis, Data curation. **Mattia Sivero:** Writing – original draft, Investigation, Formal analysis, Data curation. **Pierfrancesco Cerruti:** Writing – review & editing, Supervision. **Veronica Ambrogi:** Writing – review & editing, Supervision. **Alice Mija:** Writing – review & editing, Supervision, Conceptualization.

Declaration of competing interest

The authors declare that they have no known competing financial interests or personal relationships that could have appeared to influence the work reported in this paper.

Appendix A. Supplementary data

Supplementary data to this article can be found online at doi: mmcdoino

Data availability

Data will be made available on request.

References

[1] D.J. Ponting, M.A. Ortega, I.B. Niklasson, I. Karlsson, T. Seifert, J. Stéen, K. Luthman, A.T. Karlberg, Development of new epoxy resin monomers–a delicate balance between skin allergy and polymerization properties, Chem. Res. Toxicol. 32 (2019) 57–66, https://doi.org/10.1021/acs.chemrestox.8b00169.
[2] E.A. Baroncini, S. Kumar Yadav, G.R. Palmese, J.F. Stanzione III, Recent advances in bio-based epoxy resins and bio-based epoxy curing agents, J. Appl. Polym. Sci. 133 (2016) 44103, https://doi.org/10.1002/app.44103.
[3] J.M. España, L. Sánchez-Nacher, T. Boronat, V. Fombuena, R. Balart, Properties of biobased epoxy resins from epoxidized soybean oil (ESBO) cured with maleic anhydride (MA), J. Am. Oil Chem. Soc. 89 (2012) 2067–2075, https://doi.org/10.1007/s11746-012-2102-2.
[4] K. Huang, Z. Liu, J. Zhang, S. Li, M. Li, J. Xia, Y. Zhou, Epoxy monomers derived from tung oil fatty acids and its regulable thermosets cured in two synergistic ways, Biomacromolecules 15 (2014) 837–843, https://doi.org/10.1021/bm4018929.
[5] C. Di Mauro, T.N. Tran, A. Graillot, A. Mija, Enhancing the recyclability of a vegetable oil-based epoxy thermoset through initiator influence, ACS Sustainable Chem. Eng. 8 (2020) 7690–7700, https://doi.org/10.1021/acssuschemeng.0c01419.
[6] C. Di Mauro, S. Malburet, A. Genua, A. Graillot, A. Mija, Sustainable series of new epoxidized vegetable oil-based thermosets with chemical recycling properties, Biomacromolecules 21 (2020) 3923–3935, https://doi.org/10.1021/acs.biomac.0c01059.
[7] C. Di Mauro, A. Genua, A. Mija, Fully bio-based reprocessable thermosetting resins based on epoxidized vegetable oils cured with itaconic acid, Ind. Crops Prod. 185 (2022) 115116, https://doi.org/10.1016/j.indcrop.2022.115116.
[8] T. Liu, C. Hao, L. Wang, Y. Li, W. Liu, J. Xin, J. Zhang, Eugenol-derived biobased epoxy: shape memory, repairing, and recyclability, Macromolecules 50 (2017) 8588–8597, https://doi.org/10.1021/acs.macromol.7b01889.
[9] I. Faye, M. Decostanzi, Y. Ecochard, S. Caillol, Eugenol bio-based epoxy thermosets: from cloves to applied materials, Green Chem. 19 (2017) 5236–5242, https://doi.org/10.1039/C7GC02322G.
[10] N. Gao, Y. Lu, J. Li, F. Zhao, M. Ru, S. Zhao, S. Xiang, F. Fu, H. Diao, X. Liu, A fully degradable epoxy resin based on a nontoxic triphenol derived from diphenolic acid and eugenol, Polym. Chem. 15 (2024) 3256–3265, https://doi.org/10.1039/D4PY00599F.
[11] M. Fache, A. Viola, R. Auvergne, B. Boutevin, S. Caillol, Biobased epoxy thermosets from vanillin-derived oligomers, Eur. Polym. J. 68 (2015) 526–535, https://doi.org/10.1016/j.eurpolymj.2015.03.048.
[12] E. Savonnet, E. Grau, S. Grelier, B. Defoort, H. Cramail, Divanillin-based epoxy precursors as DGEBA substitutes for biobased epoxy thermosets, ACS Sustainable Chem. Eng. 6 (2018) 11008–11017, https://doi.org/10.1021/acssuschemeng.8b02419.
[13] X. Su, Z. Zhou, J. Liu, J. Luo, R. Liu, A recyclable vanillin-based epoxy resin with high-performance that can compete with DGEBA, Eur. Polym. J. 140 (2020) 110053, https://doi.org/10.1016/j.eurpolymj.2020.110053.
[14] R.B. Senanayake, H. Gan, J. Zhang, D. Liu, R.J. Varley, Impact of stoichiometry on the network structure, properties, and processing relationships of an epoxy tannic acid resin system, ACS Appl. Polym. Mater. 6 (2024) 2107–2117, https://doi.org/10.1021/acsapm.3c02212.
[15] C. Gioia, M.B. Banella, M. Vannini, A. Celli, M. Colonna, D. Caretti, Resorcinol: a potentially bio-based building block for the preparation of sustainable polyesters, Eur. Polym. J. 73 (2015) 38–49, https://doi.org/10.1016/j.eurpolymj.2015.09.030.
[16] I. Fusteș-Dămoc, T. Măluțan, A. Mija, Chitosan as a polyfunctional crosslinker for a renewable-based resorcinol diglycidyl ether, ACS Sustainable Chem. Eng. 11 (2023) 7605–7616, https://doi.org/10.1021/acssuschemeng.3c01429.
[17] Q.B. Nguyen, N.H. Nguyen, A. Rios de Anda, V.H. Nguyen, D.L. Versace, V. Langlois, S. Naili, E. Renard, Photocurable bulk epoxy resins based on resorcinol derivative through cationic polymerization, J. Appl. Polym. Sci. 137 (2020) 49051, https://doi.org/10.1002/app.49051.
[18] T. Modjinou, D.L. Versace, S. Abbad-Andaloussi, V. Langlois, E. Renard, Antibacterial and antioxidant photoinitiated epoxy co-networks of resorcinol and eugenol derivatives, Mater. Today Commun. 12 (2017) 19–28, https://doi.org/10.1016/j.mtcomm.2017.03.005.
[19] N. Mattar, A.R. de Anda, H. Vahabi, E. Renard, V. Langlois, Resorcinol-based epoxy resins hardened with limonene and eugenol derivatives: from the synthesis of renewable diamines to the mechanical properties of biobased thermosets, ACS

Sustainable Chem. Eng. 8 (34) (2020) 13064–13075, https://doi.org/10.1021/acssuschemeng.0c04780.
[20] R. Dinu, C. Cantarutti, A. Mija, Design of sustainable materials by cross-linking a biobased epoxide with keratin and lignin, ACS Sustainable Chem. Eng. 8 (2020) 6844–6852, https://doi.org/10.1021/acssuschemeng.0c01759.
[21] F. Jaillet, M. Desroches, R. Auvergne, B. Boutevin, S. Caillol, New biobased carboxylic acid hardeners for epoxy resins, Eur. J. Lipid Sci. Technol. 115 (2013) 698–708, https://doi.org/10.1002/ejlt.201200363.
[22] C. François, S. Pourchet, G. Boni, S. Rautiainen, J. Samec, L. Fournier, C. Robert, C. M. Thomas, S. Fontaine, Y. Gaillard, V. Placet, L. Plasseraud, Design and synthesis of biobased epoxy thermosets from biorenewable resources, C. R., Chim. 20 (2017) 1006–1016, https://doi.org/10.1016/j.crci.2017.10.005.
[23] X. Fernández-Francos, A. Rybak, R. Sekula, X. Ramis, A. Serra, Modification of epoxy–anhydride thermosets using a hyperbranched poly (ester-amide): I. Kinetic study, Polym. Int. 61 (2012) 1710–1725, https://doi.org/10.1002/pi.4259.
[24] E.V. Anslyn, D.A. Dougherty, Transition state theory and related topics, in: E. V. Anslyn, D.A. Dougherty (Eds.), Modern Physical Organic Chemistry, University Science Books, Melville, New York, 2006, pp. 365–373.
[25] K.J. Laidler, M.C. King, The development of transition-state theory, J. Phys. Chem. 87 (1983) 2657–2664, https://doi.org/10.1021/j100238a002.
[26] M. Ghaemy, M. Barghamadi, H. Behmadi, Cure kinetics of epoxy resin and aromatic diamines, J. Appl. Polym. Sci. 94 (2004) 1049–1056, https://doi.org/10.1002/app.20960.
[27] C. Li, H. Fan, J. Hu, B. Li, Novel silicone aliphatic amine curing agent for epoxy resin: 1, 3-Bis (2-aminoethylaminomethyl) tetramethyldisiloxane. 2. Isothermal cure, and dynamic mechanical property, Thermochim. Acta 549 (2012) 132–139, https://doi.org/10.1016/j.tca.2012.09.008.
[28] F. Ferdosian, Y. Zhang, Z. Yuan, M. Anderson, C. Xu, Curing kinetics and mechanical properties of bio-based epoxy composites comprising lignin-based epoxy resins, Eur. Polym. J. 82 (2016) 153–165, https://doi.org/10.1016/j.eurpolymj.2016.07.014.
[29] J. Wan, B. Gan, C. Li, J. Molina-Aldareguia, E.N. Kalali, X. Wang, D.Y. Wang, A sustainable, eugenol-derived epoxy resin with high biobased content, modulus, hardness and low flammability: synthesis, curing kinetics and structure–property relationship, Chem. Eng. J. 284 (2016) 1080–1093, https://doi.org/10.1016/j.cej.2015.09.031.
[30] M.R. Kamal, S. Sourour, Kinetics and thermal characterization of thermoset cure, Polym. Eng. Sci. 13 (1973) 59–64, https://doi.org/10.1002/pen.760130110.
[31] M.R. Kamal, Thermoset characterization for moldability analysis, Polym. Eng. Sci. 14 (1974) 231–239, https://doi.org/10.1002/pen.760140312.
[32] F.Y.C. Boey, W. Qiang, Experimental modeling of the cure kinetics of an epoxy-hexaanhydro-4-methylphthalicanhydride (MHHPA) system, Polymer 41 (2000) 2081–2094, https://doi.org/10.1016/S0032-3861(99)00409-7.
[33] U. Khanna, M. Chanda, Kinetics of anhydride curing of isophthalic diglycidyl ester using differential scanning calorimetry, J. Appl. Polym. Sci. 49 (1993) 319–329, https://doi.org/10.1002/app.1993.070490212.
[34] B. Ellis, Chemistry and Technology of Epoxy Resins, first ed., Springer Science+Business Media, 1993.
[35] C. François, S. Pourchet, G. Boni, S. Fontaine, Y. Gaillard, V. Placet, M.V. Galkin, A. Orebom, J. Samec, L. Plasseraud, Diglycidylether of iso-eugenol: a suitable lignin-derived synthon for epoxy thermoset applications, RSC Adv. 6 (2016) 68732–68738, https://doi.org/10.1039/C6RA15200G.
[36] P. Musto, E. Martuscelli, G. Ragosta, P. Russo, G. Scarinzi, An interpenetrated system based on a tetrafunctional epoxy resin and a thermosetting bismaleimide: structure–Properties correlation, J. Appl. Polym. Sci. 69 (1998) 1029–1042, https://doi.org/10.1002/(SICI)1097-4628(19980801)69:5%3C1029::AIDAPP23%3E3.0.CO;2-V.
[37] A. Marotta, N. Faggio, V. Ambrogi, P. Cerruti, G. Gentile, A. Mija, Curing behavior and properties of sustainable furan-based epoxy/anhydride resins, Biomacromolecules 20 (2019) 3831–3841, https://doi.org/10.1021/acs.biomac.9b00919.
[38] M. Rebei, O. Kočková, M. Řehák, S. Abbrent, A. Vykydalová, J. Honzíček, P. Ecorchard, H. Beneš, Accelerating effect of metal ionic liquids for epoxy-anhydride copolymerization, Eur. Polym. J. 212 (2024) 113077, https://doi.org/10.1016/j.eurpolymj.2024.113077.
[39] C. Brondi, A. Marotta, G. Filippone, G. Mensitieri, M. Salzano de Luna, V. Ambrogi, Curing behavior of reprocessable epoxy vitrimers: thermal analysis and kinetics modeling, Macromol. Chem. Phys. 224 (2023) 2300273, https://doi.org/10.1002/macp.202300273.
[40] A. Marotta, N. Faggio, C. Brondi, Curing kinetics of bioderived furan-based epoxy resins: study on the effect of the epoxy monomer/hardener ratio, Polymers 14 (2022) 5322, https://doi.org/10.3390/polym14235322.
[41] G. Sun, H. Sun, Y. Liu, B. Zhao, N. Zhu, K. Hu, Comparative study on the curing kinetics and mechanism of a lignin-based-epoxy/anhydride resin system, Polymer 48 (2007) 330–337, https://doi.org/10.1016/j.polymer.2006.10.047.
[42] A. Tomuta, F. Ferrando, A. Serra, X. Ramis, New aromatic-aliphatic hyperbranched polyesters with vinylic end groups of different length as modifiers of epoxy/anhydride thermosets, React. Funct. Polym. 72 (2012) 556–563, https://doi.org/10.1016/j.reactfunctpolym.2012.05.008.
[43] W.H. Park, J.K. Lee, K.J. Kwon, Cure behavior of an epoxy-anhydride-imidazole system, Polym. J. 28 (1996) 407–411, https://doi.org/10.1295/polymj.28.407.
[44] M.S. Heise, G.C. Martin, Curing mechanism and thermal properties of epoxyimidazole systems, Macromolecules 22 (1989) 99–104, https://doi.org/10.1021/ma00191a020.
[45] K. Dušek, S. Luňák, L. Matějka, Gelation in the curing of epoxy resins with anhydrides, Polym. Bull. 7 (1982) 145–152, https://doi.org/10.1007/BF00265465.
[46] S. Kumar, S.K. Samal, S. Mohanty, S.K. Nayak, Study of curing kinetics of anhydride cured petroleum-based (DGEBA) epoxy resin and renewable resource based epoxidized soybean oil (ESO) systems catalyzed by 2-methylimidazole, Thermochim. Acta 654 (2017) 112–120, https://doi.org/10.1016/j.tca.2017.05.016.
[47] G.C. Montanari, M. Xu, D. Fabiani, L.A. Dissado, The effect of mechanical relaxation on ultra-fast charge pulses in flexible epoxy resin nanocomposites, Appl. Phys. A 107 (2012) 539–551, https://doi.org/10.1007/s00339-012-6845-2.
[48] S.J. Park, F.L. Jin, Thermal stabilities and dynamic mechanical properties of sulfone containing epoxy resin cured with anhydride, Polym. Degrad. Stab. 86 (2004) 515–520, https://doi.org/10.1016/j.polymdegradstab.2004.06.003.
[49] S.G. Tan, W.S. Chow, Curing characteristics and thermal properties of epoxidized soybean oil based thermosetting resin, J. Am. Oil Chem. Soc. 88 (2011) 915–923, https://doi.org/10.1007/s11746-010-1748-x.
[50] L.R. Amirova, O.L. Khamidullin, K.A. Andrianova, L.M. Amirova, Thermal properties of epoxy–anhydride formulations cured using phosphonium accelerators, Polym. Bull. 75 (2018) 5253–5267, https://doi.org/10.1007/s00289-018-2330-1.
[51] N. Boquillon, C. Fringant, Polymer networks derived from curing of epoxidised linseed oil: influence of different catalysts and anhydride hardeners, Polymer 41 (2000) 8603–8613, https://doi.org/10.1016/S0032-3861(00)00256-1.
[52] N. Faggio, A. Marotta, V. Ambrogi, P. Cerruti, G. Gentile, Fully bio-based furan/maleic anhydride epoxy resin with enhanced adhesive properties, J. Mater. Sci. 58 (2023) 7195–7208, https://doi.org/10.1007/s10853-023-08458-8.
[53] S. Kocaman, G. Ahmetli, A study of coating properties of biobased modified epoxy resin with different hardeners, Prog. Org. Coating 97 (2016) 53–64, https://doi.org/10.1016/j.porgcoat.2016.03.025.